Inorg. Chem. **1991**, *30*, 3948-3955

Contribution from the Departments of Chemistry and Physics, Jadavpur University, Calcutta 700 032, India, and Department of Solid State Physics, Indian Association for the Cultivation of Science, Calcutta 700 032, India

Reaction of MoO_4^{2-} and WO_4^{2-} with Aqueous Polysulfides: Synthesis, Structure, and Electrochemistry of η^2-Polysulfido Complexes Containing a Bridging S,S $\{M_2O_2S_2\}^{2+}$ (M = Mo, W) Core

Ramgopal Bhattacharyya,[*,1a] Prasanta K. Chakrabarty,[1a] Pradip N. Ghosh,[1a] Alok K. Mukherjee,[1b] Debi Podder,[1b] and Monika Mukherjee[1c]

Received January 25, 1991

Aqueous molybdate and polysulfide solution when cooked together for 3 h affords $R_2[Mo_2O_2S_2(S_2)(S_4)]$, where R = Me_4N (**3a**), Et_4N (**3b**), and Ph_4P (**3c**) cations. Tungstate solution however needs to be reduced to oxotungsten(V) before polysulfide treatment to get the compounds $R'_2[W_2O_2S_2(S_2)(S_4)]$ [R' = Me_4N (**4**)] and $R''_2[W_2O_2S_2(S_4)_2]$ [R'' = Et_4N (**5a**), Ph_4P (**5b**)]. A ν_{S-S} band above 500 cm^{-1} in the Raman spectrum is diagnostic for complexes containing the S_2^{2-} ligand, while two such bands, one at ~420 cm^{-1} and the other at ~490 cm^{-1}, are diagnostic for the S_4^{2-} ligand. The M-M interaction in the compounds is evident from their observed diamagnetism and is further supported by Mo-Mo and W-W distances of ca. 2.83 Å in **3b** (crystal data: a = 14.993 (4) Å, b = 12.397 (3) Å, c = 15.825 (4) Å, β = 92.29 (3)°, monoclinic $P2_1/a$, Z = 4, R = 0.045) and **4**. The complex anion in **3b** contains a discrete $\{Mo_2O_2S_2\}^{2+}$ core coordinated by η^2-S_2 and η^2-S_4 ligands, and the coordination geometry about the Mo atoms can be described as that of two square pyramids sharing an edge containing bridging S,S ligands. In the electronic spectrum, a band above 400 nm has been found to be characteristic of an $M(S_2)$ three-membered-ring system. The position of Mo $3d_{5/2,3/2}$ and W $4f_{7/2,5/2}$ is typical for pentavalent Mo and W, respectively, in a sulfur environment. An interesting aspect of the electrochemical study of the $\{M_2O_2S_2\}^{2+}$ core in DMF is the observation of reversible or quasireversible cyclic responses showing step by step reduction (for M = Mo) of two Mo(V) centers to Mo(IV), the reverse scan also showing corresponding oxidation steps. In the case of M = W, unless at slow scan, the reduction is a 2-electron single-step process, the reverse sweep exhibiting two-step single-electron oxidative responses.

Introduction

Molybdenum and tungsten, the 4d and 5d congeners of the so-called sub group VI elements (presently group 6) in the periodic table, have much of a common chemistry. But, the reactivities of MoO_4^{2-} and WO_4^{2-} are very much different. The facile reducibility of MoO_4^{2-}, as against WO_4^{2-}, especially toward NH_2OH and polysulfide ions, gave way to a rich Mo-NO and Mo-S cluster chemistry.[2] The main reason for this is a favorable redox potential of $Mo^{VI} \rightarrow Mo^{V}$, compared to that of the W analogue.[3] Metal-sulfur aggregates and clusters, in general, have received continued interest in recent times for their rampancy in bio- and geospheres.[4] Relevance of Mo-S compounds to bioinorganic chemistry is well-known,[5] but the role of tungsten in biology is, nonetheless, also important.[6] Interest in M-S (M = Mo, W) chemistry has also grown due to the implication of the metals in catalysis, especially in HDS (hydrodesulfurization) reactions.[7] However, albeit an in-depth study on reaction of MoS_4^{2-} with sulfur or polysulfide ions leading to the isolation of a wide range of stable chain Mo-S anions, viz., $Mo_2S_8^{2-}$,[8] $Mo_2O_2S_6^{2-}$,[9] $Mo_2OS_7^{2-}$,[10] $Mo_2O_2S_9^{2-}$,[11] $Mo_2S_{10}^{2-}$,[12] $Mo_2S_{12}^{2-}$,[13] $Mo_3S_9^{2-}$,[14] $Mo_3OS_8^{2-}$,[15] and $Mo_3O_2S_8^{2-}$,[16] all that is known about the reaction of S_x^{2-} with MoO_4^{2-} is the products obtained, viz., $(NH_4)_2[Mo_3S(S_2)_6]$ (**1**) and $(NH_4)_2[Mo_2(S_2)_6]$ (**2**), after a prolonged boiling or standing of the reactants.[17] Herein is reported for the first time[18] the synthesis and structural characterization of the products, $R_2[Mo_2O_2S_8]$ [R = Me_4N (**3a**), Et_4N (**3b**), Ph_4P (**3c**)], obtained by reacting a solution of MoO_4^{2-} and S_x^{2-} and then precipitating the complex anion by using relevant countercations.

With tungsten, however, a much less extensive set of structurally well-defined thio- and oxothiometalates have been reported, viz., $W_3S_9^{2-}$,[19] $W_3S_8^{2-}$,[20] $W_3OS_8^{2-}$,[21] $W_2S_{10}^{2-}$,[22] $W_4S_{12}^{2-}$,[23] and $W_3S_{10}^{2-}$.[24] Notwithstanding the establishment of $\{W_2S_4\}^{2+}$ core structure in some recently known W-S systems[22,23] the $\{W_2O_2S_2\}^{2+}$ moiety is extremely rare contrary to the ample examples of the corresponding Mo analogue.[25] Besides a brief and preliminary conference abstract,[26] there is only one well-documented example[27]

---

(1) (a) Department of Chemistry, Jadavpur University. (b) Department of Physics, Jadavpur University. (c) Indian Association for the Cultivation of Science.

(2) Cotton, F. A.; Wilkinson, G. *Advanced Inorganic Chemistry*, 4th ed.; John Wiley and Sons, Inc.: New York, 1980.

(3) Latimer, W. M. *The Oxidation States of the Elements and Their Potentials in Aqueous Solution*, 2nd ed.; Prentice-Hall: New York, 1952.

(4) Krauskopf, K. B. *Introduction to Geochemistry*; McGraw-Hill: New York, 1979. Halbert, T. R.; Hutchings, R. R.; Stiefel, E. I. *J. Am. Chem. Soc.* **1986**, *108*, 6437-6438 and references cited therein. Müller, A.; Diemann, E.; Jostes, R. Naturwissenschaften **1984**, *71*, 420-421.

(5) (a) Stiefel, E. I. *Prog. Inorg. Chem.* **1977**, *22*, 1-223. (b) Swedo, K. B.; Enemark, J. H. *J. Chem. Educ.* **1979**, *56*, 70-76.

(6) Yamamoto, I.; Saiki, T.; Liu, S. M.; Ljungdhal, L. G. *J. Biol. Chem.* **1983**, *258*, 1826-1832.

(7) (a) Massoth, F. E. *Adv. Catal.* **1978**, *87*, 265. (b) Stiefel, E. I.; Chianelli, R. R. In *Nitrogen Fixation, The Chemical-Biochemical-Genetic Interface*; Müller, A., Newton, W. E., Eds.; Plenum Press: New York, 1983.

(8) Pan, W. H.; Harmer, M. A.; Halbert, T. R.; Stiefel, E. I. *J. Am. Chem. Soc.* **1984**, *106*, 459-460.

(9) Clegg, W.; Mohan, N.; Müller, A.; Neumann, A.; Rittner, W.; Sheldrick, G. M. *Inorg. Chem.* **1980**, *19*, 2066-2069.

(10) Xin, X. Q.; Morris, N. L.; Jameson, G. B.; Pope, M. T. *Inorg. Chem.* **1985**, *24*, 3482-3485.

(11) Coucouvanis, D.; Hadjikysiacou, A. *Inorg. Chem.* **1987**, *26*, 1-2.

(12) Clegg, W.; Christou, G.; Garner, C. D.; Sheldrick, G. M. *Inorg. Chem.* **1981**, *20*, 1562-1566.

(13) (a) Müller, A.; Nolte, W. O.; Krebs, B. *Angew. Chem., Int. Ed. Engl.* **1978**, *17*, 279. (b) Müller, A.; Nolte, W. O.; Krebs, B. *Inorg. Chem.* **1980**, *19*, 2835-2836.

(14) Pan, W. H.; Leonowicz, M. E.; Stiefel, E. I. *Inorg. Chem.* **1983**, *22*, 672-678.

(15) Müller, A.; Hellmann, W.; Römer, C.; Römer, M.; Bögge, H.; Jostes, R.; Schimanksi, U. *Inorg. Chim. Acta* **1984**, *83*, L75-L77.

(16) Xin, X. Q.; Jin, G. X.; Wang, B.; Pope, M. T. *Inorg. Chem.* **1990**, *29*, 553-554.

(17) Müller, A.; Bhattacharyya, R. G.; Pfefferkorn, B. *Chem. Ber.* **1979**, *112*, 778-780.

(18) While preparing this manuscript, we noticed a report of the synthesis of **3b**; however, see, for instance: Coucouvanis, D.; Toupadakis, A.; Hadjikysiacou, A. *Inorg. Chem.* **1988**, *27*, 3272-3273.

(19) Müller, A.; Bhattacharyya, R. G.; Koniger-Ahlborn, E.; Sharma, R. C.; Rittner, W.; Neumann, A.; Henkel, G.; Krebs, B. *Inorg. Chim. Acta* **1979**, *37*, L493.

(20) Bhaduri, S.; Ibers, J. A. *Inorg. Chem.* **1986**, *25*, 3-4.

(21) Müller, A.; Bogge, H.; Krikemeyer, E.; Hankel, G.; Krebs, B. *Z. Naturforsch. B: Anorg. Chem. Org. Chem.* **1982**, *37B*, 1014-1019.

(22) Müller, A.; Römer, M.; Römer, C.; Reinsch-Vogell, U.; Bögge, H.; Schimanski, U. *Monatsh. Chem.* **1985**, *116*, 711-716.

(23) Secheresse, F.; Lefebvre, J.; Daran, J. C.; Jeannin, Y. *Inorg. Chem.* **1982**, *21*, 1311-1314.

(24) Müller, A.; Diemann, E.; Weinbeker, U.; Bögge, H. *Inorg. Chem.* **1989**, *28*, 4046-4049.

(25) Müller, A.; Bhattacharyya, R. G.; Mohan, N.; Pfefferkorn, B. *Z. Anorg. Allg. Chem.* **1979**, *454*, 118-124. See also ref 9.

0020-1669/91/1330-3948$02.50/0

(i.e. existing in $[W_2O_2S_2Cl_4]^{2-}$) of its kind.[28] The present paper also reports the generation of the moiety I in the form of anionic

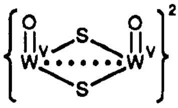

I

complexes ligated with η^2-S_2^{2-} and η^2-S_4^{2-}, viz., $(Me_4N)_2[W_2O_2S_8]$ (**4**) and $R'_2[W_2O_2S_{10}]$ [R′ = Et_4N (**5a**), Ph_4P (**5b**)], or a neutral complex $[W_2O_2S_2(DEDTC)_2]$ (**6**) (DEDTC = diethyldithiocarbamate anion).

Experimental Section

Materials. All chemicals used in this work were of GR (E. Merck, FRG) grade. Acetonitrile used for spectroscopic and other physicochemical studies was further purified by treatment with CaH_2 (overnight) followed by successive distillation over Li_2CO_3–$KMnO_4$ and P_4O_{10}.[29] All other solvents required for various purposes were further purified by the literature method[30] before use. The solvents were stored over molecular sieves (4 Å). Commercial tetraethylammonium chloride was converted to pure tetraethylammonium perchlorate (TEAP) by following an available procedure.[31] Dinitrogen gas was purified by successively bubbling it through alkaline dithionite and concentrated sulfuric acid. Triple distilled water (all glass) was used throughout the work. Aqueous ammonium polysulfide solution was prepared as described earlier.[32]

Physical Measurements. Spectroscopic data were obtained by using the following instruments: IR (CsI or polyethylene disk; 4000–200 cm^{-1}), Perkin-Elmer 597 spectrophotometer; Raman (50–1150 cm^{-1}; solid sample; rotating cell technique), Spex Ramanlog 5M or Coderg T800 instrument equipped with a coherent CR4 (λ_e = 488.0 and 514.5 nm) or CR 500K (λ_e = 647.1 nm) laser; electronic spectra (2600–200 nm), Hitachi Model U 3400 UV-vis-near-IR spectrophotometer. The X-ray photoelectron spectra were recorded by using an ESCALAB 503 spectrometer with vacuum generators. The Al K α line (1486.6 eV) was used as the excitation source. The spectra were calibrated by using the Cl $s_{1/2}$ binding energy (at 285.0 eV) from pump oil as an internal standard. A Phillips Model PW 1730/1710C XRD system (Cu Kα radiation) was used for measuring *d*-spacings. Solution electrical conductances were measured by using a Systronics (India) Model 335 digital conductivity bridge. Electrochemical measurements were done by using a PAR Model 378-1 electrochemistry system incorporating the following components: 174A, polarographic analyzer; 175, universal programmer; RE0074, XY recorder; 173 potentiostat; 377, cell system. All experiments were performed under a dinitrogen atmosphere. A stout platinum-wire working electrode, a platinum-foil auxiliary electrode, and an aqueous saturated calomel reference electrode (SCE) were used in the three-electrode configuration. All electrochemical data were collected at 298 K and are uncorrected for junction potentials. Coulometry was performed in a 273 potentiostat/galvanostat using a 377 cell system equipped with Pt wire gauge working electrode. EPR scanning was done in a Varian B 109C spectrometer equipped with a quartz dewar for measuring at 77 K. The elements C, H, and N were analyzed microanalytically by using a Perkin-Elmer 240C elemental analyzer, and Mo, W, S and P, by conventional gravimetric [Mo as MoO_2 (8-quinolinolate)$_2$, W as WO_3, S as $BaSO_4$, and P as P_2O_5·$24MoO_3$] methods.[33]

Preparation of Complexes. Molybdenum Complexes. $(NH_4)_6Mo_7O_{24}$·$4H_2O$ (10 g; 0.057 mol of Mo) was dissolved in 80 mL of aqueous NH_4OH (1:1), and to the solution was added 300 mL of aqueous $(NH_4)_2S_x$. The resulting solution was kept on a boiling water bath for 3–4 h when a red-brown solution was obtained. The solution was filtered, if necessary, and then divided into four equal portions.

Table I. Crystallographic Data for $(Et_4N)_2[Mo_2O_2S_2(S_2)(S_4)]$ (**3b**)

chem formula $Mo_2O_2S_8N_2C_{16}H_{40}$	space group $P2_1/a$ (No. 14)
a = 14.993 (4) Å	λ = 0.71073 Å
b = 12.397 (3) Å	ρ_{obsd} = 1.67 g cm^{-3},
c = 15.825 (4) Å	ρ_{calcd} = 1.674 g cm^{-3}
β = 92.29 (3)°	μ = 13.1 cm^{-1}
V = 2939 (1) $Å^3$	transm coeff = 0.961–0.702
Z = 4	$R(F_o)$ = 0.045
T = 18 °C	$R_w(F_o)$ = 0.050
fw 740.9	

$(Me_4N)_2[Mo_2O_2S_2(S_2)(S_4)]$ (3a). To the portion 1, an aqueous (10 mL) solution of Me_4NCl (3.0 g, 0.028 mol) was added with stirring and brownish red product separated out, which was filtered off, washed with water, ethanol, carbon disulfide, and ether. The product was crystallized from an acetone–light petroleum (40–60 °C) mixture. Yield: 3.5 g (80%). Anal. Calcd for $C_8H_{24}N_2Mo_2O_2S_8$: C, 15.3; H, 3.8; N, 4.4; S, 40.7; Mo, 30.6. Found: C, 14.8; H, 3.8; N, 4.2; S, 39.8; Mo, 30.4.

$(Et_4N)_2[Mo_2O_2S_2(S_2)(S_4)]$ (3b). To the portion 2 was added an aqueous solution (10 mL) of Et_4NCl (5.0 g; 0.030 mol), and a yellow-brown product that separated was worked up as above. Yield: 2.0 g (40%). Anal. Calcd for $C_{16}H_{40}N_2Mo_2O_2S_8$: C, 26.0; H, 5.4; N, 3.8; S, 34.6; Mo, 26.0. Found: C, 26.1; H, 5.6; N, 3.8; S, 34.1; Mo, 26.5.

$(PPh_4)_2[Mo_2O_2S_2(S_2)(S_4)]$ (3c). To the portion of 3, an aqueous solution (30 mL) of Ph_4PCl (11.2 g, 0.030 mol) was added as a precipitant, and the product was worked up as usual. Yield: 7.5 g (93%). Anal. Calcd for $C_{48}H_{40}P_2Mo_2O_2S_8$: C, 49.7; H, 3.5; P, 5.4; S, 22.1; Mo, 16.6. Found: C, 50.0; H, 3.6; P, 5.8; S, 22.2; Mo 16.9.

$(NH_4)_2[Mo_2S_{12}]$·$2H_2O$ (2). To the portion 4, H_2S was passed for 3 h when a deep brown-black crystalline product of the known compound $(NH_4)_2[Mo_2S_{12}]$·$2H_2O$ separated out, which was filtered off, washed with 2-propanol, CS_2, and finally with diethyl ether. Yield: 4.2 g (92%). Anal. Calcd for $H_{12}N_2O_2Mo_2S_{12}$: N, 4.3; H, 1.9; S, 59.3; Mo, 29.6. Found: N, 4.4; H, 2.1; S, 59.0; Mo, 30.0.

Tungsten Complexes. A mixture of sodium tungstate (Na_2WO_4·$2H_2O$; 15 g, 0.045 mol) and NH_4SCN (35 g, 0.450 mol) was dissolved in 6 M HCl (400 mL) while being stirred with a stir bar in a 1-L beaker. Stirring was continued for 1.5 h, i.e., until a deep green color appeared. The green solution was filtered, and to the filtrate, taken in a 2-L Erlenmeyer flask, sufficient $(NH_4)_2S_x$ solution (400 mL) was added dropwise with stirring until the violent and exothermic reaction ceased. The orange-red solution obtained was filtered out and divided into three equal portions.

$(Me_4N)_2[W_2O_2S_2(S_2)(S_4)]$·$Me_2CO$ (4). To the portion 1, an aqueous solution (25 mL) of Me_4NCl (15 g; 0.135 mol) was added when a reddish orange precipitate appeared. The solid was filtered off, washed with water, ethanol, CS_2, and diethyl ether, and vacuum-dried. The crude product was crystallized from an acetone–light petroleum (40–60 °C) mixture. The yield was 2.5 g (70%). Anal. Calcd for $C_{11}H_{30}N_2W_2O_3S_8$: C, 15.3; H, 3.5; N, 3.3; S, 29.7; W, 42.7. Found: C, 15.5; H, 3.4; N, 3.3; S, 30.0; W, 42.3.

$(Et_4N)_2[W_2O_2S_2(S_4)_2]$ (5a). To the portion 2, an aqueous solution (25 mL) of Et_4NCl (5 g; 0.030 mol) was added and worked up as above. Yield: 2.1 g (30%). Anal. Calcd for $C_{16}H_{40}N_2W_2O_2S_{10}$: C, 19.6; H, 4.1; N, 2.9; S, 32.7; W, 37.6. Found: C, 19.9; H, 4.2; N, 3.0; S, 32.4; W, 37.2.

$(Ph_4P)_2[W_2O_2S_2(S_4)_2]$ (5b). To the portion 3, and aqueous solution (30 mL) of Ph_4PCl (11.2 g; 0.030 mol) was added, and a yellow solid separated. It was filtered off and worked up as above when an orange-yellow microcrystalline product was obtained. Yield: 3 g (29%). Anal. Calcd for $C_{48}H_{40}P_2W_2O_2S_{10}$: C, 41.2; H, 2.9; P, 4.4; S, 22.9; W, 26.3. Found: C, 41.4; H, 3.1; P, 4.3; S, 22.3; W, 25.9.

$[W_2O_2S_2(DEDTC)_2]$ (6). The method applied to **5a** was used except with NaDEDTC·$3H_2O$ instead of Et_4NCl, and a yellow compound separated. The substance was vacuum-dried after a nonexceptional workup. Yield: 2 g (35%). The crude product was crystallized from chloroform–ether mixture. Anal. Calcd for $C_{10}H_{20}N_2W_2O_2S_6$: C, 15.8; H, 2.6; N, 3.7; S, 25.3; W, 48.4. Found: C, 15.7; H, 2.8; N, 3.9; S, 24.8; W, 48.0.

Crystal Structure Determination of $(Et_4N)_2[Mo_2O_2S_2(S_2)(S_4)]$ (3b). Summaries of the crystal data and data collection parameters are listed in Table I. A single crystal of **3b**, obtained by slow crystallization from acetonitrile–ether (1:1) solvent mixture, was mounted on a glass fiber with an adhesive. Intensity data were collected on a Nicolet R 3m/V automated diffractometer using graphite-monochromated Mo Kα radiation (λ = 0.71073 Å). Unit cell parameters were obtained by least-

---

(26) Bhattacharyya, R. G.; Rai-Choudhuri, A. In *Proceedings of the XIII International Conference on Coordination Chemistry*, Boulder, CO, 1984; TH_p 54-4.

(27) Drew, M. G. B.; Page, E. M.; Rice, D. A. *Inorg. Chim. Acta* **1983**, *76*, L33–L34.

(28) A report (Sarkar, S.; Ansari, M. A. *J. Chem. Soc., Chem. Commun.* **1986**, 324–325) claims to have synthesized (hitherto unrepeatable by us) the product already described in ref 26.

(29) (a) Sawyer, D. T.; Roberts, J. L., Jr. *Experimental Electrochemistry for Chemists*; Wiley: New York, 1974; pp 167. (b) Walter, M.; Ramaley, L. *Anal. Chem.* **1973**, *45*, 165–166.

(30) Perrin, D. D.; Armerego, W. L. F.; Perrin, D. R. *Purification of Laboratory Chemicals*; Pergamon: New York, 1966.

(31) Goswami, S.; Chakravarty, A. R.; Chakravorty, A. *Inorg. Chem.* **1982**, *21*, 2737–2742.

(32) Müller, A.; Bhattacharyya, R. G.; Eltzner, W.; Mohan, N.; Neumann, A.; Sarkar, S. In *Proceedings of the Climax Third International Conference on the Chemistry and Uses of Molybdenum*; Barry, H. F., Mitchell, P. C. H., Eds.; Climax Molybdenum Co.: Ann Arbor, MI, 1979. See also ref 17.

(33) Vogel, A. I. *A Text Book of Quantitative Inorganic Analysis*; The English Language Book Society and Longmans: London, 1968.

Table II. Atom Coordinates of $(Et_4N)_2[Mo_2O_2S_2(S_2)(S_4)]$ (**3b**)

atom	*x*/*a*	*y*/*b*	*z*/*c*
Mo1	0.1515 (1)	−0.0576 (1)	0.7919 (1)
Mo2	0.3122 (1)	0.0586 (1)	0.7758 (1)
S1	0.0701 (3)	−0.2001 (3)	0.7225 (2)
S2	0.0006 (2)	−0.0576 (3)	0.7382 (3)
S3	0.1637 (2)	0.1217 (2)	0.7602 (2)
S4	0.3241 (2)	0.2310 (2)	0.7067 (2)
S5	0.4485 (3)	0.2536 (3)	0.6548 (3)
S6	0.5240 (2)	0.1392 (3)	0.7130 (2)
S7	0.4434 (2)	0.0048 (3)	0.7018 (2)
S8	0.2852 (2)	−0.1245 (2)	0.7461 (2)
O1	0.1486 (5)	−0.0745 (6)	0.8959 (5)
O2	0.3459 (5)	0.0721 (6)	0.8780 (5)
N1	0.2300 (6)	0.0828 (6)	0.4447 (5)
N2	0.9182 (6)	0.7420 (6)	0.9971 (5)
C1	0.3179 (10)	0.1393 (13)	0.4562 (11)
C2	0.2108 (13)	0.0176 (12)	0.5212 (10)
C3	0.2371 (11)	0.0053 (11)	0.3698 (11)
C4	0.1597 (10)	0.1626 (11)	0.4287 (14)
C5	0.4013 (9)	0.0760 (14)	0.4648 (10)
C6	0.1261 (11)	−0.0418 (12)	0.5237 (11)
C7	0.2642 (12)	0.0530 (12)	0.2902 (9)
C8	0.1367 (11)	0.2348 (12)	0.4971 (10)
C9	0.8559 (9)	0.6477 (10)	1.0038 (9)
C10	0.9696 (9)	0.7263 (10)	0.9194 (9)
C11	0.9782 (8)	0.7463 (11)	1.0752 (8)
C12	0.8667 (10)	0.8477 (9)	0.9900 (9)
C13	0.7930 (10)	0.6504 (11)	1.0757 (10)
C14	1.0302 (9)	0.6281 (11)	0.9181 (8)
C15	1.0456 (9)	0.8404 (12)	1.0783 (10)
C16	0.7944 (12)	0.8481 (13)	0.9234 (12)

squares refinement of the angular settings of 20 reflections having 2θ range 10–25°. Intensities of three standard reflections monitored after every 97 reflections did not show any appreciable decay during data collection. An empirical absorption correction[34] was applied. The data were corrected for Lorentz and polarization effects.

The positions of the two Mo atoms were determined from a Patterson map, and the remaining non-hydrogen atoms were located from successive difference-Fourier maps. The structure was refined by full-matrix least-squares methods using program SHELX.[35] In the final cycles of refinement all non-hydrogen atoms were made anisotropic while the hydrogen atoms were held fixed in the geometrically calculated positions with isotropic thermal parameters. The highest peak in the last difference-Fourier map was 0.72 e/Å^3. The atomic scattering factors for all atoms were taken from standard sources.[36] Anomalous dispersion corrections were applied to Mo and S atoms. Atomic coordinates are given in Table II. All computations were performed on a Cyber 180/840A system at the Regional Computer Centre, Calcutta, India.

Results and Discussion

A. Synthetic Aspects. Tetraoxomolybdate(VI) ions were known to react with S_x^{2-} in aqueous alkaline medium at an elevated temperature for 15 h to afford $[Mo_3S_{13}]^{2-}$ (**1**) and $[Mo_2S_{12}]^{2-}$ (**2**) as NH_4 salts.[17] This reaction when conducted for a shorter time (3–4 h) and when the existing complex anion is precipitated with counterions produces hitherto unknown $R_2[Mo_2O_2S_2(S_2)(S_4)]$ [R = Me_4N (**3a**), Et_4N (**3b**), Ph_4P (**3c**)]. Interestingly, **3a**, **3b**, and **3c** are always isolable from the solution phase up to the point immediately before the NH_4 salts **1** and **2** start precipitating. From this reaction mixture never could $[Mo_2O_2S_2(S_2)_2]^{2-}$, $[Mo_2O_2S_2(S_4)_2]^{2-}$, $[Mo_2S_4(S_x)_2]^{2-}$ (x = 2, 4, or any other number) or any other all-sulfido–molybdenum derivative be isolated. However, after the same 3–4 h of cooking, if H_2S gas is passed through the reaction mixture, almost a quantitative yield of the crystals $(NH_4)_2[Mo_2S_{12}]\cdot 2H_2O$ (**2**) is obtained as evidenced by the superimposable IR spectra and X-ray powder diffractogram with the authenticated sample[17] of the compound. Uptil now, this is the quickest and the most efficient method for the synthesis of **2**. Also $DEDTC^-$ yields under the same medium the well-known $[Mo_2O_2S_2(DEDTC)_2]$. All these observations indicate that the $\{Mo_2O_2S_2\}^{2+}$ moiety exists in the reaction medium for a long time, and the method is a very convenient way to generate the binuclear S,S-bridged oxomolybdenum(V) moiety.[37] WO_4^{2-} is not reducible with S_x^{2-}, and so the same has been reduced to a green WO^{3+} species by using NCS^-/H^+.[38] This oxotungsten(V) species reacts with S_x^{2-} immediately, and the addition of counterions to the reaction mixture leads to the precipitation of $(Me_4N)_2[W_2O_2S_2(S_2)(S_4)]$ (**4**) and $R_2''[W_2O_2S_2(S_4)_2]$ [R″ = Et_4N (**5a**), Ph_4P (**5b**)]. It may be noted that contrary to the molybdenum case, here the complex compositions are cation dependent. Again, a passage of H_2S through the above reaction mixture does not give $(NH_4)_2[W_2S_{12}]$ (different from Mo), and the tungsten analogues of **1** and **2** are not obtainable even on long heating. However, the moiety I, existing in the reaction solution, can be trapped with $DEDTC^-$, affording $[W_2O_2S_2(DEDTC)_2]$ (**6**). The reaction sequence for Mo and W is shown in Scheme I.

Scheme I

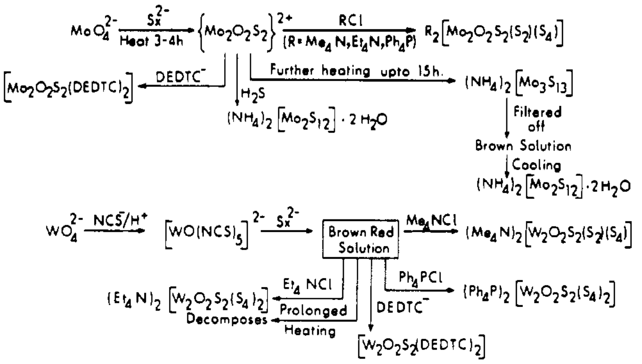

B. General Characterization and Vibrational Spectroscopy. All the complexes excepting **6** (a nonelectrolyte) behave quite expectedly, as 2:1 electrolytes in CH_3CN (Table III). All the compounds are grossly diamagnetic, but the molybdenum complexes show a feeble paramagnetism (ca. 0.5 μ_B) after diamagnetic corrections for ligands. The diamagnetism obviously indicates the existence of a metal–metal bond in these dimeric Mo(V) and W(V) (d^1) systems, which is confirmed by three-dimensional X-ray crystallographic studies.

The observation of a split $\nu_{M=O}$ vibration at ca. 950 cm^{-1} (Table III) and a $\nu_{as(MS_2M)}$ (i.e. the asymmetric MS_2M bridging vibration) vibration at ca. 450 cm^{-1} in the infrared spectrum with the corresponding symmetric vibration appearing quite expectedly only in the Raman spectrum at ca. 460 cm^{-1} (for the exact position, see Table III) clearly demonstrate the presence of moiety I (with W = M) in all the complexes studied. These types of IR and Raman bands are actually a diagnostic feature[25,39] of the said moiety, as revealed by similar studies in analogous Mo complexes.[40] The ν_{S-S} vibration due to S_2^{2-} or S_4^{2-} coordination to the metal ions is obtained in the IR spectrum at ca. 520 cm^{-1}, but in the Raman spectrum the S_4^{2-} ligands show two very prominent absorptions, one at ca. 420 cm^{-1} and other at ca. 490 cm^{-1}, while S_2^{2-} absorbs only at ca. 510 cm^{-1}. In the present case the absence of S_2^{2-} in **5a** and **5b** is clearly demonstrated by the presence of both the S_4^{2-} vibrations mentioned above but the lack of any vibrational band above 500 cm^{-1}. Similarly, the presence of both S_4^{2-} and S_2^{2-} in **3a–c** and **4** is demonstrated by the conspicuous appearance of bands at ~420 and ~490 cm^{-1}, as well as at ~510 cm^{-1}. These Raman vibrations may be used as diagnostic features of coordinated S_2^{2-} and S_4^{2-} moieties.[41,42]

---

(34) North, A. C. T.; Phillips, D. C.; Mathews, F. S. *Acta Crystallogr.* **1968**, *A24*, 351–359.

(35) Sheldrick, G. M. SHELX 76, Program for crystal structure determination, University of Cambridge, England, 1976.

(36) *International Tables for X-ray crystallography*; Kynoch Press: Birmingham, England, 1974; Vol. IV.

(37) A fourthcoming publication of ours will describe the complexes of the type $[Mo_2O_2S_2(LL)_2]$, where LL = bidentate monoanionic N, O; N, S; O, S; or S, S donor organic ligands.

(38) Funk, H.; Böhland, H. *Z. Anorg. Allg. Chem.* **1962**, *318*, 169–175. Bhattacharyya, R. G. Unpublished work.

(39) Newton, W. E.; Mcdonald, J. W. *J. Less-Common Met.* **1977**, *54*, 51–62.

(40) Dirand-Colin, J.; Schappacher, M.; Ricard, L.; Weiss, R. *J. Less-Common Met.* **1977**, *54*, 91–99.

Table III. Vibrational Spectroscopic and Solution Conductance Data

compd	selected vibrational spectroscopic data, cm^{-1}						molar conductance in CH_3CN, Ω^{-1} cm^2 M^{-1}
	type	$\nu_{M=O}$	ν_{S-S}	$\nu_{as(MS_2M)}$[a]	$\nu_{S(MS_2M)}$[a]	$\nu_{(M-S)_t}$[b]	
$(Me_4N)_2[Mo_2O_2S_8]$ (**3a**)	IR	950 (s) 940 (sh)	515 (m)	460 (m) 320 (w)		360 (w)	250
	R	948 (m)	510 (m) 496 (m) 418 (m)		460 (m)	340 (w)	
$(Et_4N)_2[Mo_2O_2S_8]$ (**3b**)	IR	950 (s) 940 (m)	520 (m)	460 (m) 320 (m)		360 (w)	250
	R	945 (m)	518 (m) 493 (m) 418 (m)		459 (m)	358 (w)	
$(Ph_4P)_2[Mo_2O_2S_8]$ (**3c**)	IR	950 (s) 940 (m)	*c*	460 (m) 320 (w)		350 (w)	240
	R	942 (m)	521 (m) 493 (m) 420 (m)		459 (m)	358 (w)	
$(Me_4N)_2[W_2O_2S_8]\cdot Me_2CO$ (**4**)	IR	950 (s) 940 (sh)	520 (m)	450 (m)		340 (w)	250
	R	947 (m) 927 (w)	509 (m) 495 (m) 423 (m)		456 (m)	340 (w)	
$(Et_4N)_2[W_2O_2S_{10}]$ (**5a**)	IR	950 (s) 940 (m)	515 (m)	440 (m)		320 (w) 310 (w)	260
	R	955 (m)	497 (m) 412 (m)		463 (w)	340 (w)	
$(Ph_4P)_2[W_2O_2S_{10}]$ (**5b**)	IR	950 (s) 940 (m)	*c*	440 (m) 435 (w)		320 (w)	240
	R	960 (m)	497 (m) 414 (m)		461 (w)	322 (w)	
$[W_2O_2S_2(DEDTC)_2]$[d] (**6**)	IR	965 (s) 975 (sh)		440 (m) 320 (m)		365 (m)	*e*
	R	970 (m)			450 (m)	360 (m)	

[a] The vibration of the corresponding four-membered ring. [b] Due to $M-S_x$ linkage. [c] Masked by the PPh_4 absorption. [d] $\nu_{C=N}$ at 1530 cm^{-1} (s). [e] Nonelectrolyte.

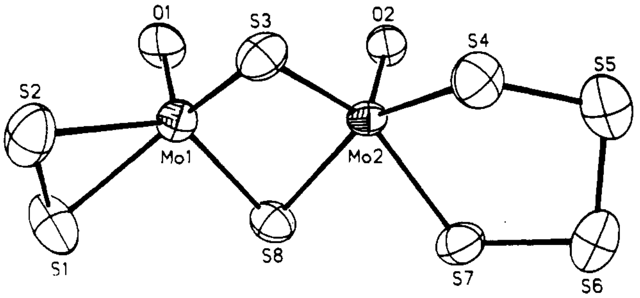

Figure 1. ORTEP view of the $[Mo_2O_2S_2(S_2)(S_4)]^{2-}$ anion of **3b**, giving the atom-labeling scheme used.

Table IV. Selected Bond Distances (Å) and Angles (deg) in $(Et_4N)_2[Mo_2O_2S_2(S_2)(S_4)]$ (**3b**)

	Distances		
Mo1–S1	2.389 (3)	Mo2–S3	2.364 (3)
Mo1–S2	2.385 (4)	Mo2–S8	2.349 (3)
Mo1–S3	2.288 (3)	Mo2–S4	2.411 (3)
Mo1–S8	2.312 (3)	Mo2–S7	2.422 (3)
Mo1–O1	1.663 (7)	Mo2–O2	1.684 (7)
S1–S2	2.071 (5)	S4–S5	2.088 (5)
S5–S6	2.014 (6)	S6–S7	2.062 (5)
Mo1–Mo2	2.827 (1)		
	Angles		
S1–Mo1–S2	51.4 (1)	S3–Mo2–S4	75.2 (1)
S1–Mo1–S3	131.4 (1)	S3–Mo2–S7	145.1 (1)
S1–Mo1–S8	91.4 (1)	S3–Mo2–S8	98.3 (1)
S1–Mo1–O1	109.2 (3)	S4–Mo2–S7	87.1 (1)
S2–Mo1–O1	106.9 (3)	S4–Mo2–S8	141.4 (1)
S2–Mo1–S3	90.3 (1)	S4–Mo2–O2	108.8 (3)
S2–Mo1–S8	135.3 (1)	S7–Mo2–S8	76.9 (1)
S3–Mo1–S8	101.7 (1)	S7–Mo2–O2	105.9 (3)
S3–Mo1–O1	110.2 (3)	S8–Mo2–O2	109.3 (3)
S8–Mo1–O1	108.8 (3)	Mo2–S7–S6	102.7 (2)
Mo1–S3–Mo2	74.8 (1)	Mo2–S4–S5	112.3 (2)
Mo1–S8–Mo2	74.7 (1)	S4–S5–S6	102.7 (2)
S3–Mo2–O2	108.2 (3)	S5–S6–S7	102.3 (2)

C. Molecular Structure of $(Et_4N)_2[Mo_2O_2S_2(S_2)(S_4)]$ (3b) and the Structural Aspects of Other Compounds. The crystal structure of **3b** consists of discrete $[Mo_2O_2S_2(S_2)(S_4)]^{2-}$ anions and Et_4N^+ cations. An ORTEP[43] view of the anion with the atom-labeling scheme is shown in Figure 1. Selected bond distances and angles are listed in Table IV. The anion $[Mo_2O_2S_8]^{2-}$ contains a $\{Mo_2O_2S_2\}^{2+}$ core coordinated by η^2-S_2 and η^2-S_4 ligands. The skeleton geometry of the anion is similar to those of other molybdenum complexes[8,9,12,44,45] containing $\{Mo_2X_2S_2\}^{2+}$ cores, where X = S or O (Table V). The coordination geometry about the molybdenum atoms in **3b** is best described as that of two square pyramids sharing a common basal edge formed by the S3 and S8 atoms. Both the molybdenum atoms in $[Mo_2O_2S_8]^{2-}$ are bonded to four sulfur ligands and one oxygen ligand in a distorted square-pyramidal arrangement with Mo1 atom 0.764 (2) Å away from the basal plane defined by S1, S2, S3, and S8 [Mo2 atom is away by 0.740 (2) Å from the plane through S3, S4, S7, and S8; the dihedral angle between the two basal planes is 22.1 (1)°]. The apical oxygen–molybdenum distances for **3b** (Table IV) are comparable with those observed in similar structures containing terminal oxygen–molybdenum multiple-bond distances: $[N(CH_3)_4]_2[Mo_2O_2S_6]$,[9] 1.68 (1) Å; $[Mo_2O_2S_4(DMF)_3]$,[18] 1.686 (6) Å; $(Ph_4P)_2[Mo_2O_2S_{10}]$,[46] 1.69 (2) Å; $[(C_4H_9)_4N]_2[Mo_3O_2S_8]$,[16]

---

(41) Baumann, F. W. Diplom Arbeit (M.S. Thesis), University of Bielefeld, Bielefeld, FRG, 1984.

(42) Eltzner, W. Ph.D. Dissertation, University of Bielefeld, Bielefeld, FRG, 1984.

(43) Johnson, C. K. ORTEP; Oak Ridge National Laboratory: Oak Ridge, TN, 1965.

(44) Cohen, S. A.; Stiefel, E. I. *Inorg. Chem.* **1985**, *24*, 4657–4662.

(45) Coucouvanis, D.; Koo, S.-M. *Inorg. Chem.* **1989**, *28*, 2–5.

(46) Müller, A. *Polyhedron* **1986**, *5*, 323–340.

Table V. Structural Data[a] for Selected Anions Containing the $\{Mo_2X_2S_2\}^{2+}$ Core, Where X = S or O

anion	M–M, Å	$M–S_b$,[b] Å	$M–S_\alpha$,[b] Å	$S_b–M–S_b$, deg	ref
$[Mo_2O_2S_2(S_2)(S_4)]^{2-}$	2.827 (1)	2.300 (3)	2.387 (3)[c]	101.7 (1)	this work
		2.356 (3)	2.416 (3)[d]	98.3 (1)	
$[Mo_2S_4(S_2)_2]^{2-}$	2.821 (1)	2.314 (4)	2.394 (14)	101.2 (2)	8
$[Mo_2S_4(S_4)(S_2)]^{2-}$	2.837 (1)	2.296 (10)	2.394 (2)[c]	100.7 (1)	12
		2.342 (13)	2.406 (4)[d]	103.4 (1)	
$[Mo_2O_2S_2(S_2)_2]^{2-}$	2.825 (2)	2.324 (4)	2.410 (5)[c]	101.8 (2)	9
$[Mo_2OS_7]^{2-}$	2.820 (1)	2.319 (2)	2.393 (3)[c]		45

[a] The average values of chemically equivalent and crystallographically independent bond lengths and angles are given. [b] S_b and S_α represents bridging and terminal sulfur atoms, respectively. [c] Metal bonded to S_2^{2-} ligand. [d] Metal bonded to S_4^{2-} ligand.

Table VI. Electronic Spectral Data for the Complex Anions in Acetonitrile Medium

compd	bandhead, nm	molar abs ϵ, M^{-1} cm^{-1}
$(Me_4N)_2[Mo_2O_2S_8]$ (**3a**)	270, 320, 390, 480	1200, 1800, 600, 900
$(Et_4N)_2[Mo_2O_2S_8]$ (**3b**)	265, 320, 390, 480	1040, 2600, 780, 1040
$(Ph_4P)_2[Mo_2O_2S_8]$ (**3c**)	*a*, 315, 390, 480	2860, 780, 1040
$(Me_4N)_2[W_2O_2S_8]$ (**4**)	290, 380, 438	4000, 240, 160
$(Et_4N)_2[W_2O_2S_{10}]$ (**5a**)	285, 390	3300, 300
$(Ph_4P)_2[W_2O_2S_{10}]$ (**5b**)	315, 390	3500, 480
$W_2O_2S_2(DEDTC)_2$[b] (**6**)	305, 335, 415	4000, 500, 100

[a] Buried under strong PPh_4^+ absorption. [b] In chloroform.

1.691 (4) Å. The bridging sulfur atoms are asymmetrically bonded to the molybdenum atoms, and S_b–Mo distances and S_b–Mo–S_b angles ranging between 2.288 (3) and 2.364 (3) Å and 98.3 (1) and 101.7 (1)° agree well with the corresponding parameters for structures containing similar cores (Table V). The asymmetry of the S_b–Mo1 bonds compared to the S_b–Mo2 ones (Table IV) is reported for similar complexes of molybdenum (Table V) and tungsten[22] where the central core $\{M_2X_2S_2\}^{2+}$ (M = Mo, W; X = O, S) is coordinated by different ligands as in **3b**. The bond distances and angles involving molybdenum and terminal sulfur atoms (S1, S2, S4, S7) are within the ranges observed for related structures (Table V). The Et_4N^+ cations are of usual geometry and the structural data for the cations are given in Table SII (supplementary material). No unusual short contacts are observed.

From the X-ray powder diffractogram the calculated *d*-spacings and their intensities are recorded in Table SIII (supplementary material). It clearly shows that **3a** is isostructural with **4** as is also confirmed by single-crystal structural characterization.[47] It is noteworthy that the powder diffraction pattern of **5b** is identical with that of the structurally characterized compound prepared otherwise,[22] thereby confirming the structural prediction of the molecule from analytical and spectroscopic data. So the structure of the anions of **4** and **5a,b** can be represented as in Figure 2.

D. Electronic Aspects. (a) Electronic Spectral Studies. The complexes containing at least one three-centered $M(S_2)$ core are found to furnish a band above 400 nm (for the exact position, see Table VI), which may be assigned to the $\pi^* \rightarrow \sigma^*$[d(metal)] LMCT transition. Obviously,[14] the band is at higher energy in the case of tungsten (i.e. complex **4**) than in that of the molybdenum complexes (Table VI). The corresponding $\pi_h^* \rightarrow d$ transition is expected at a much lower wavelength region,[48-51] and the band around 270 nm in the cases of the Mo complexes may be assigned to this. The band around 290 nm in the tungsten complexes is not assignable to this transition insofar as the same should be expected[14] at a lower wavelength than that of the Mo analogue. It is quite interesting to note that the band above 400 nm is absent in the complexes containing only S_4^{2-} ligands coordinated to the $\{Mo({=}O)S_2M({=}O)\}^{2+}$ core and the presence of this band is diagnostic (like the 500-cm^{-1} vibrational band in the Raman spectrum) of the existence of S_2^{2-} ligand in the metal complexes and helps to detect coordinated S_2^{2-} in the presence of higher polysulfido ligands also. The band at 390 nm is common to all compounds containing S_4^{2-} and probably is an intraligand transition localized on this moiety. The 320-nm band in Mo and the ca. 300-nm band in W complexes may be due to the charge transfer from $S_{bonding} \rightarrow (M{=}O)_t$ antibonding orbital, insofar as the charge-transfer band involving the $(M{=}S)_t$ analogue is known to occur at a higher wavelength.[48] The 415-nm band in **6** is assignable to a S(DEDTC) → W LMCT transition.

(b) X-ray Photoelectron Spectroscopy. The S 2p binding energies of the isolated complexes are shown in the Table VII. Slight differences existing in the S 2p binding energies are hardly significant to be attributed to any interesting electronic effect insofar as variation of cations can also cause such a meager change in binding energies. However, the obtained Mo $3d_{5/2,3/2}$ and W $4f_{7/2,5/2}$ binding energy values quoted in Table VII indicate the +5 oxidation state of the respective metal ions in a sulfur environment.[48,51]

E. Electrochemistry. All the isolated complexes show reversible, quasi-reversible, and irreversible oxidation and reduction behavior in their cyclic voltammograms in DMF (*N,N'*-dimethylformamide) TEAP medium. In the potential range of −0.4 to −1.5 V vs SCE interesting reversible or quasi-reversible cyclic voltammetric responses, centered on the $\{M_2O_2S_2\}^{2+}$ (M = Mo, W) moiety,[52-55] are exhibited (Figure 3, showing **3b** and **5a** as representative cases) especially at a higher scan rate. The Mo complexes **3a–c** at scan rates of 50 and 100 mV s^{-1} show two successive reductive responses, one at ca. −0.86 V and the other at ca. −1.38 V vs SCE, and in the reverse sweep the corresponding oxidation peaks are obtained at ca. −1.30 V for the latter and ca. −0.80 V for the former. At higher scan rates the two reductive peaks come closer to each other (ca. −0.90 and −1.26 V vs SCE) and at the same time the first peak becomes less prominent. Exhaustive electrolysis (coulometry) at a constant potential (−1.50 V vs SCE) gives a coulomb count commensurate with a two-electron change (i.e. one electron per Mo center in all the cases), and the electrolyzed solution is EPR silent. Also very controlled coulometry at a potential of −1.0 V vs SCE shows the transient existence[56] of

---

(47) Müller, A.; Bögge, H. Private communication. Due to a marked disorder and other problems, the structure of **5a** could be refined only up to *R* = 0.129, and the details are not publishable at this stage. However, as also mentioned in the text, the tetraphenylphosphonium salt of the complex anion, i.e. **5b**, has herein been structurally characterized by observing a superimposable powder diffraction pattern with that of the structurally characterized complex prepared otherwise (see ref 22). The structure of **4** (showing a W–W distance of 2.83 Å) on the other hand, where no disorder problem exists, has been refined to *R* = 0.074. For details of the structure of **4**, see: Müller, A.; Bögge, H. University of Bielefeld, Bielefeld, FRG.

(48) (a) Müller, A.; Jaegermann, W.; Enemark, J. H. *Coord. Chem. Rev.* **1982**, *46*, 245–280 and references cited therein. (b) Müller, A.; Jaegermann, W. *Inorg. Chem.* **1979**, *18*, 2631–2633.

(49) Lever, A. B. P.; Gray, H. B. *Acc. Chem. Res.* **1978**, *11*, 348–355.

(50) (a) Tuck, D. G.; Walters, R. H. *Inorg. Chem.* **1963**, *2*, 428–429. (b) Secheresse, F.; Manoli, J. M.; Potvin, C. *Inorg. Chem.* **1986**, *25*, 3967–3971.

(51) Müller, A.; Jostes, R.; Eltzner, W.; Nie, C.-S.; Diemann, E.; Bögge, H.; Zimmermann, M.; Dartmann, M.; Reinsch-Vogell, U.; Che, S.; Cyvin, S. J.; Cyvin, B. N. *Inorg. Chem.* **1985**, *14*, 2872–2884. Diemann, E.; Muller, A.; *Chem. Phys. Lett.* **1974**, *27*, 351–354.

(52) Howlader, N. C.; Haight, G. P., Jr.; Hambley, T. W.; Snow, M. R.; Lawrance, G. A. *Inorg. Chem.* **1984**, *23*, 1811–1815.

(53) Ott, V. R.; Swieter, D. S.; Schultz, F. A. *Inorg. Chem.* **1977**, *16*, 2538–2545.

(54) Schultz, F. A.; Ott, V. R.; Rolison, D. S.; Bravard, D. C.; Mcdonald, J. W.; Newton, W. E. *Inorg. Chem.* **1978**, *17*, 1758–1765 and references cited therein.

(55) Unoura, K.; Ooi, T.; Tanaka, K.; Iwase, A. *J. Electroanal. Chem. Interfacial Electrochem.* **1988**, *252*, 335–343.

Table VII. X-ray Photoelectron Spectroscopic Data for the Isolated Compounds

compd	E_b, eV S 2p	Mo $3d_{5/2}$/W $4f_{7/2}$	Mo $3d_{3/2}$/W $4f_{5/2}$	N 1s	O 1s
$(Et_4N)_2[Mo_2O_2S_8]$ (**3b**)	162.4	230.8	234.1	402.0	531.2
$(Ph_4P)_2[Mo_2O_2S_8]$ (**3c**)	162.6	230.3	233.5	187.8[a] 133.1[b]	531.1
$(Me_4N)_2[W_2O_2S_8]$ (**4**)	162.3	33.4	35.4	402.2	530.8
$(Et_4N)_2[W_2O_2S_{10}]$ (**5a**)	162.6	33.8	35.7	402.1	531.4
$(Ph_4P)_2[W_2O_2S_{10}]$ (**5b**)	162.6	33.8	35.6	188.0[a] 133.2[b]	531.4

[a] P 2s binding energy. [b] P 2p binding energy.

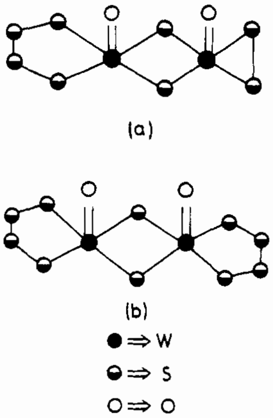

Figure 2. Molecular structure of (a) $[W_2O_2S_2(S_2)(S_4)]^{2-}$ (**4**) and (b) $[W_2O_2S_2(S_4)_2]^{2-}$ (**5a-b**).

one-electron reduced species, but the resulting solution was also not found to be EPR active. Notably the total current height of the anodic peaks (i_a) is a bit higher than that of the cathodic peaks (i_c), the ratio being ca. 1.1, and at higher scan rates the oxidative peaks draw proportionately more current. The above facts indicate the presence of the electrochemical equilibria (1) and (2) in the Mo complexes. These types of sequential one-electron redox steps

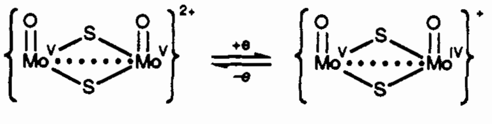

(1)

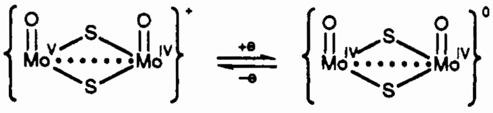

(2)

in nonaqueous medium had been observed by previous workers where the $\{Mo_2O_2S_2\}^{2+}$ core was again ligated with S-donor ligands, viz., dithiocarbamate,[52] cystein,[53] and 1,1-dithiolates.[54] Those groups of workers also observed that the first process (eq 1) becomes more reversible at fast scan rates in the systems studied by them. But in the present cases, as stated earlier, the first reductive step is rather slow and is observed at scan rates of 50 and 100 mV s^{-1}. At higher scan rates (200, 500 mV s^{-1}) the wave appears merely as an inflection and it is the second process that shows prominency and reversibility at the cost of the first one. This is borne out by the ΔE_p values of the observed cyclic responses. The details of electrochemical data with reference to SCE as well as to F_c (ferrocene)–F_c^+ (ferrocenium), where necessary, are listed in Table VIII, depicting the effect of different scan rates.

The tungsten compounds **4**, **5a**, **5b** at the scan rates 100, 200, and 500 mV s^{-1} show a reductive response at −1.30 V, and the reverse sweeps show two oxidation steps at ca. −0.76 and −1.22

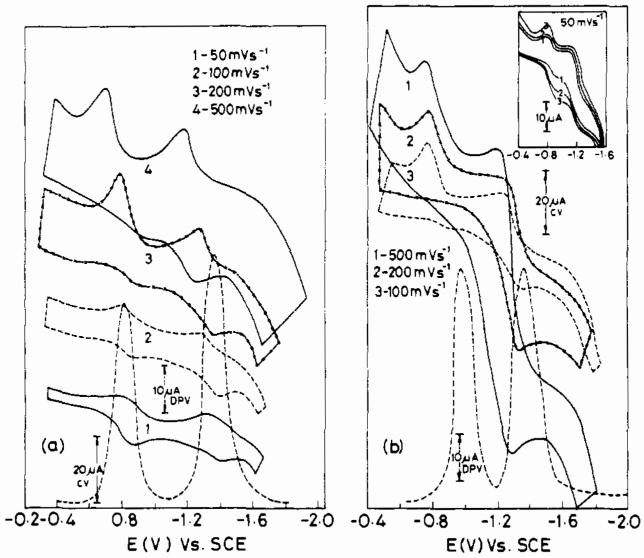

Figure 3. Segmented cyclic voltammograms in the scan rates of 50–500 mV s^{-1} in DMF (0.1 M TEAP) at a platinum electrode vs SCE: (a) CV's of $(Et_4N)_2[Mo_2O_2S_2(S_2)(S_4)]$ (**3b**); (b) CV's of $(Et_4N)_2[W_2O_2S_2(S_4)_2]$ (**5b**). The CV of **5b** at a scan rate 50 mV s^{-1} is shown in the inset of (b), where 1–3 indicate the first, second, and third scan, respectively. The solution concentration in each case is $\sim 10^{-3}$ M. Differential pulse voltammograms (DPV's) of **3b** and **5a** in the scan rate 5 mV s^{-1} are shown in (a) and (b), respectively.

V, respectively (Figure 3, citing **5a** as a representative case). The reductive response is essentially a single-step two-electron-transfer process (ensured by controlled-potential coulometry at −1.50 V), thereby suggesting the electrochemical reactions shown in eqs 3–5 take place. Here the i_a/i_c ratio obtained by dividing the total

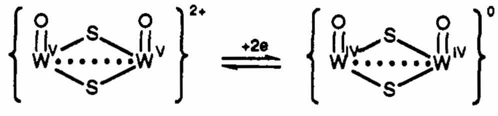

(3)

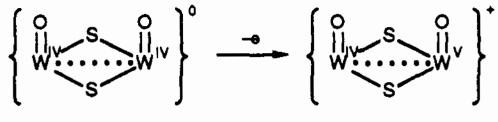

(4)

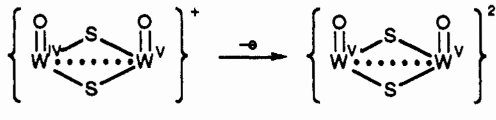

(5)

current heights of two anodic peaks with that of one cathodic peak is a bit higher than unity. However, a CV scan at 50 mV s^{-1} and a differential-pulse voltammetric (DPV) study at 5 mV s^{-1} (Figure 3) show two reduction peaks indicating stepwise reduction, i.e., $W^V_2 \rightleftharpoons W^VW^{IV}$, $W^VW^{IV} \rightleftharpoons W^{IV}_2$. Evidently, here, the first process is much slower than that of the Mo cases, and the said peak grows in with continued cycling but positionally approaching closer to the second peak. Hence, at slow scan rate there does not exist any essential difference in the electrochemistry of the

---

(56) The rate of coulomb absorption decreases for a while and then again increases briskly; the rate of absorption for the second electron is decidedly higher than that of the first electron.

Table VIII. Cyclic Voltammetric Data for the Isolated Complexes[a] in the Range of 0.0 to −1.6 V under DMF/TEAP Medium

		reversible or quasi-reversible potential V vs SCE[b]			
compd	scan rate, mV s^{-1}	E_c(redn)	E_a(oxidn)	$E°_{298}$[c]	ΔE_p, mV
$(Me_4N)_2[Mo_2O_2S_8]$ (**3a**)	50	−0.86	−0.80	−0.83 (−1.28)	60
		−1.36	−1.28	−1.32 (−1.77)	80
	100	−0.86	−0.78	−0.82 (−1.27)	80
		−1.34	−1.26	−1.30 (−1.75)	80
	200	−0.88	−0.76	−0.82 (−1.27)	120
		−1.30	−1.22	−1.26 (−1.71)	80
	500	−0.90[d]	−0.70	−0.80 (−1.25)	200
		−1.27	−1.20	−1.24 (−1.69)	70
$(Et_4N)_2[Mo_2O_2S_8]$ (**3b**)	50	−0.86	−0.80	−0.83 (−1.28)	60
		−1.38	−1.30	−1.34 (−1.79)	80
	100	−0.86	−0.78	−0.82 (−1.27)	80
		−1.38	−1.30	−1.34 (−1.79)	80
	200	−0.88	−0.76	−0.82 (−1.27)	120
		−1.36	−1.28	−1.32 (−1.77)	80
	500	−0.92[d]	−0.72	−0.82 (−1.27)	200
		−1.26	−1.20	−1.23 (−1.68)	60
$(Ph_4P)_2[Mo_2O_2S_8]$ (**3c**)	50	−0.84	−0.78	−0.81 (−1.26)	60
		−1.38	−1.28	−1.33 (−1.78)	100
	100	−0.86	−0.76	−0.81 (−1.26)	100
		−1.36	−1.28	−1.32 (−1.77)	80
	200	−0.88	−0.74	−0.81 (−1.26)	100
		−1.36	−1.28	−1.32 (−1.77)	80
	500	−0.92[d]	−0.72	−0.82 (−1.27)	200
		−1.26	−1.20	−1.23 (−1.68)	60
$(Me_4N)_2[W_2O_2S_8]$ (**4**)	50	*e*	−0.8		
		−1.32	−1.22	−1.28 (−1.73)	100
	100	*e*	−0.8		
		−1.32	−1.22	−1.27 (−1.72)	100
	200	*e*	−0.76		
		−1.30	−1.22	−1.26 (−1.71)	80
	500	*e*	−0.74		
		−1.30	−1.22	−1.26 (−1.71)	80
$(Et_4N)_2[W_2O_2S_{10}]$ (**5a**)	50	−0.96	−0.80	−0.88 (−1.33)	160
		−1.36	−1.20	−1.28 (−1.73)	160
	100	−1.10[d]	−0.76	−0.93 (−1.38)	340
		−1.32	−1.20	−1.26 (−1.71)	120
	200	*e*	−0.76		
		−1.30	−1.20	−1.25 (−1.70)	100
	500	*e*	−0.74		
		−1.28	−1.20	−1.24 (−1.69)	80
$(Ph_4P)_2[W_2O_2S_{10}]$ (**5b**)	50	−1.00	−0.78	−0.89 (−1.34)	220
		−1.34	−1.22	−1.28 (−1.73)	120
	100	−1.12[d]	−0.76	−0.94 (−1.39)	360
		−1.32	−1.22	−1.27 (−1.72)	100
	200	*e*	−0.74		
		−1.30	−1.20	−1.25 (−1.70)	100
	500	*e*	−0.72		
		−1.29	−1.20	−1.25 (−1.70)	90

[a] For $[W_2O_2S_2(DEDTC)_2]$ (**6**) two reduction peaks appear at −1.88 and −2.2 V, respectively, and for $(Ph_4P)_2S_4$ three reduction peaks appear at −1.18, −1.76, and −1.96 V (for PPh_4^+). [b] The $E°_{298}$ values with reference to $[Fe(\eta\text{-}C_5H_5)_2]$–$[Fe(\eta\text{-}C_5H_5)_2]^+$ are shown in the parentheses. [c] $E°_{298} = (E_c + E_a)/2$, where E_a = potential on anodic sweep and E_c = potential on cathodic sweep. [d] Only a small inflection appears. [e] No peak appears.

$\{Mo_2O_2S_2\}^{2+}$ and $\{W_2O_2S_2\}^{2+}$ cores. A possible electrode surface contamination is not the reason for the slow kinetics of the first wave in both Mo and W cases, since substitution of a platinum electrode by a glassy-carbon one gives essentially the same results. It is noteworthy, as against a rich electrochemistry of $[Mo_2O_2S_2(DEDTC)_2]$, the tungsten analogue shows total electroinactivity at the metal center.

No metal-centered oxidation peak as reported in the analogous EDTA complex[55] is observed here. In all cases except **6** a high-current irreversible oxidation wave is observed at ca. +0.76 V (coulomb count is rather meager compared to a one-electron change) and the reduction counterpart appears at ca. −0.66 V. Both peaks are mutually interdependent. These responses may be centered on ligands. Again, an irreversible reduction peak always (except **6**) appears at ca. −1.8 V and the oxidation peak on the reverse scan occurs at ca. −0.30 V. Interestingly in W complexes, a green color is developed at the vicinity of the working platinum or glassy-carbon electrode when the reductive forward scan is extended up to −2.00 V and the color disappears on reverse sweep. These responses may be centered on S_4^{2-} ligands, since $(Ph_4P)_2S_4$ also shows similar behavior.[57]

Acknowledgment. We thank the Department of Science and Technology (DST), Government of India, for financial assistance including a fellowship to P.K.C. We are thankful to Dr. D. Ray and Mr. S. Bhanjachaudhury for X-ray data collection, partial structure solution, and ORTEP plotting carried out at the National Single Crystal Diffractometer facility established by the DST, Government of India, in the Department of Inorganic Chemistry, Indian Association for the Cultivation of Science, Calcutta, India, under Prof. A. Chakravorty, whom we also thank for providing us with the EPR facilities. Our thanks are due to the Alexander von Humboldt Foundation for the donation of the PE 597 IR spectrophotometer and to Prof. A. Müller (Bielefeld, FRG) for Raman spectra and XPS data and for letting us know the mo-

---

(57) The catalytic effect of the tungsten–sulfur center in the generation of the blue S_3^- radical (Clark, R. J. H.; Cobbold, D. G. *Inorg. Chem.* **1978**, *11*, 3169–3174) and green S_3^{2-} is under study (Bhattacharyya, R. G. Unpublished results). See also: Chivers, T.; Hojo, M. *Inorg. Chem.* **1984**, *23*, 2738–2742.

lecular structure of the W compounds. The X-ray powder diffractograms have been obtained by courtesy of the Department of Geological Sciences of this University.

Supplementary Material Available: Tables SI-SV, containing crystal data for **3b**, complete angles and distances, X-ray powder diffraction data, anisotropic thermal parameters for non-hydrogen atoms, and the derived hydrogen positions (7 pages); a table of calculated and observed structure factors (9 pages). Ordering information is given on any current masthead page.

Notes

Contribution from the Departments of Chemistry,
University of Virginia, Charlottesville, Virginia 22901,
Vanderbilt University, Nashville, Tennessee 37235,
and James Madison University, Harrisonburg, Virginia 22807

Luminescence Spectroscopy of Dinuclear Platinum Complexes Containing Bridging Alkenylidene Ligands

LouAnn Sacksteder,[1a] Eduardo Baralt,[1b] B. A. DeGraff,*,[1c] C. M. Lukehart,*,[1b] and J. N. Demas*,[1a]

Received January 15, 1991

There has been a long-standing interest in luminescent Pt complexes. Until recently, most of the attention has focused on mononuclear complexes. However, the discovery of the tetrakis(μ-pyrophosphito)diplatinum anion $Pt_2(P_2O_5H_2)_4^{4-}$ ($Pt_2(POP)_4^{4-}$) has led to the development of a group of remarkably efficient luminescent materials based on binuclear Pt complexes.[2] Thus far, to our knowledge, these materials have been restricted to systems where the central core remains two stacked square-planar Pt(II) centers held together by four POP ligands.

Earlier, we reported on the first example of a luminescent binuclear Pt(II) complex (**1** of Figure 1) where the two Pt atoms are nonequivalent and did not involve the Pt^{II}POP basic structural unit. Further, this complex is an organometallic complex with a bridging phenylethenylidene ligand, phenyl-substituted vinylidene, which possesses considerable π-bonding character. Despite the disparate structures of the two classes of compounds, similar photochemistry is observed. Theoretical calculations predict similarity between the electronic structures of complex **1** and the well-studied $Pt_2(POP)_4^{4-}$, and although the geometries of the two complexes are quite different, complex **1** exhibits photochemical reactivity similar to that observed for $Pt_2(POP)_4^{4-}$.[3]

Because of the paucity of examples of luminescent dinuclear Pt(II) complexes, we were encouraged to explore this type of complex in greater depth. We report here the results of this study and present a number of new, interesting examples of luminescent complexes involving a basic planar $Pt_2C{=}C$ chromophore unit. Further, our studies have provided some insight into the structural features that govern the photophysical processes of these complexes. We present some guidelines that could serve as the basis for further work to enhance the luminescence properties of these compounds.

Experimental Section

Synthesis. All reactions were performed under dry, prepurified nitrogen. Solvent purification procedures, spectroscopic methods, microanalytical services, and reagent preparation have been published previously.[4-6] References to the syntheses of the complexes are noted in Table I. All of the complexes except **2** are unresolved isomer pairs depending on the position of the phenyl group.

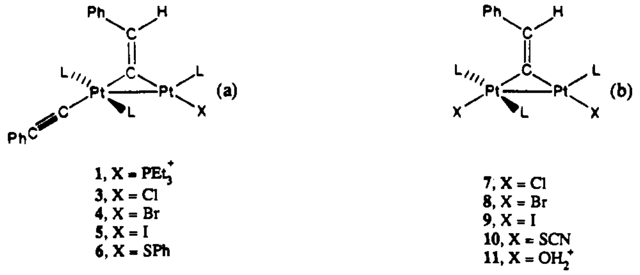

Figure 1. Structural representation of complexes (a) **1** and **3-6** and (b) **7-11**.

The structures of the complexes studied are shown in Figure 1. Except for **11** and **12**, the complexes reported here were prepared from $[Pt_2(\mu\text{-}C{=}CHY)(C{\equiv}CY)(PEt_3)_4]BF_4$ (Y = Ph (**1**) or H (**2**)) by nucleophilic substitution using procedures described previously.[3]

$[Pt_2(C{=}CHPh)(PEt_3)_3(OH_2)_2](BF_4)_2$ (**11**) was prepared by addition of 0.25 mmol of $AgBF_4$ to a stirred solution of 0.1 mmol of $Pt_2(C{=}CHPh)(C{\equiv}CPh)(PEt_3)_3Br_2$ in 10 mL of CH_2Cl_2. The solution was stirred at 25 °C for 30 min and underwent a color change from orange to deep red. The solution was filtered through Celite, and the solvent was removed at reduced pressure. The complex was isolated as a red-brown solid (76%) that became an oil upon exposure to air: mp 67-69 °C; ^1H NMR ($CDCl_3$) δ 1.23 (m, 27, CH_3), 2.05 (m, 18, CH_2), 5.8 (s, 1, CHPh), 7.30 (m, 3, para Ph, meta Ph) 8.00 (d, 2, ortho Ph, J = 8.7 Hz); $^{31}P\{^1H\}$ NMR (5% $CDCl_3$/$CHCl_3$) δ 21.5 (broad s, 3, PEt_3, $^1J_{PtP}$ = 2130.984 Hz). Anal. Calcd for $C_{26}H_{51}O_2P_3Pt_2(H_2O)_2$: C, 29.56; H, 5.24; P, 8.79. Found: C, 29.59; H, 5.46; P, 8.94.

Photophysical Studies. Room-temperature absorption spectra were recorded by using a Hewlett-Packard 8452A diode-array spectrophotometer. Emission and excitation spectra were recorded on a Spex Fluorolog 2 spectrofluorometer. Emission spectra were corrected for solvent background and instrument response. Low-temperature (77 K) spectra were recorded from 4:1 ethanol-methanol glass matrices by using an optical Dewar sample holder.

Luminescence quantum yields, Φ, were measured at low temperature by the Parker-Rees method[7,8] using $[Ru(bpy)_3]Cl_2$ (bpy = 2,2'-bipyridine) [Φ 0.376][9] as a standard. The quantum yields are the averages of at least two sets of seven measurements with the sample being removed and replaced in the sample holder for every other measurement. Room-temperature absorption spectra were used for sample optical densities, which leads to an estimated ±30% uncertainty on the low-temperature yields.

Excited-state lifetimes (τ) were measured by using a pulsed N_2 laser (337 nm) nanosecond decay system, and software described elsewhere.[10] The same optical Dewar used for emission spectra was used as the sample holder for the lifetime measurements. The nonexponential decays were fit by nonlinear least-squares[11] methods to the sum of two exponentials (eq 1), where $I(t)$ is the luminescence intensity at time t and the K's and

$$I(t) = K_s \exp(-t/\tau_s) + K_l \exp(-t/\tau_l) \qquad (1)$$

τ's are the preexponential weighting factors and the excited-state life-

---

(1) (a) University of Virginia. (b) Vanderbilt University. (c) James Madison University.

(2) Zipp, Arden P. *Coord. Chem. Rev.* **1988**, *84*, 47.

(3) Baralt, E.; Boudreaux, E. A.; Demas, J. N.; Lenhert, P. G.; Lukehart, C. M.; McPhail, A. T.; McPhail, D. R.; Myers, J. B., Jr.; Sacksteder, L.; True, W. R. *Organometallics* **1989**, *8*, 2417-2430.

(4) Afzal, D.; Lenhart, P. G.; Lukehart, C. M. *J. Am. Chem. Soc.* **1984**, *106*, 3050-3052.

(5) Lukehart, C. M.; True, W. R. *Organometallics* **1988**, *7*, 2387-2393.

(6) Afzal, D.; Lukehart, C. M. *Organometallics* **1987**, *6*, 546-550.

(7) Parker, C. A.; Rees, W. T. *Analyst (London)* **1962**, *87*, 83.

(8) Demas, J. N.; Crosby, G. A. *J. Phys. Chem.* **1971**, *75*, 991.

(9) Demas, J. N.; Crosby, G. A. *J. Am. Chem. Soc.* **1971**, *93*, 2841.

(10) (a) Turley, T. J. M.S. Thesis, University of Virginia, 1980. (b) Turley, T. J.; Demas, J. N. *Anal. Chim. Acta* **1987**, *197*, 121. (c) Sacksteder, LouAnn; Demas, J. N.; DeGraff, B. A. *Inorg. Chem.* **1989**, 1787.

(11) (a) Demas, J. M. *Excited State Lifetime Measurements*; Academic: New York, 1983. (b) Demas, J. N.; Demas, S. E. *Interfacing and Scientific Computing on Personal Computers*; Allyn & Bacon: New York, 1990.

(12) Baralt, E.; Lukehart, C. M.; McPhail, A. T.; McPhail, D. R. *Organometallics* **1991**, *10*, 516.

0020-1669/91/1330-3955$02.50/0